Coupled Mesoscale Modeling of the Ocean Wave/Atmosphere Interface Under High-Wind Speed Conditions

James D. Doyle

Naval Research Laboratory, Monterey, CA, USA

1. Introduction

The exchange of heat, momentum and moisture between the air and sea has long been recognized as a fundamental process in the development of a number of mesoscale atmospheric phenomena such as tropical cyclones, extratropical cyclones, boundary layer jets, coastal fronts, and precipitating systems. Numerical prediction of these phenomena is often critically dependent on the fidelity of surface flux representation. This air-sea exchange takes place at the fluid interface in the wave boundary layer (WBL), which underscores the potential importance of ocean waves in air-sea interaction processes.

The conventional representation of the surface roughness effects over the sea due to ocean waves, based on the scaling arguments of Charnock (1955), is used by nearly all atmospheric research and operational models, and is strictly valid only for fully-developed ocean wave conditions. Under high-wind conditions, however, wind direction and speed are often time dependent, such as for a translating tropical cyclone or topographically driven flows in the coastal zone. In these fetch-limited conditions, surface ocean waves have an increasingly important impact on the momentum flux in the atmospheric and oceanic boundary layers (Donelan 1990). In situations when the wave age is small, the wave-induced stress comprises a significant fraction of the total stress. A number of previous studies using field measurements have documented this dependence of the atmospheric momentum flux on the ocean wave age (e.g., Smith et al. 1992). The interaction between the sea and air is especially complex at high wind speeds where flux exchange processes may be impacted by sea spray and spume (Kepert et al. 1999).

Wave-induced stress may be a significant component of the total momentum stress in the atmospheric boundary layer over the ocean (e.g., Donelan 1990; Janssen 1991) and has been suggested to enhance the decay of extratropical systems (e.g., Doyle 1995). However, the impact of wind-generated ocean waves on the structure and evolution of mesoscale phenomena that are primarily forced by i) air-sea fluxes such as tropical cyclones, and ii) orography have received considerably less attention. In this study, three tropical cyclones and a Bora event are investigated using NRL's Coupled Ocean-Atmosphere Mesoscale Prediction System (COAMPS) coupled with the Wave Model (WAM) to examine the significance of coupling on the mesoscale.

2. Numerical model description

The atmospheric model used in this study is NRL's COAMPS (Hodur 1997; Hodur and Doyle 1999). Finite-difference approximations are used in the model to represent the fully compressible, nonhydrostatic equations that govern atmospheric motions. The equations are solved in three dimensions, with a nested-grid mesh capability, using a terrain-following vertical coordinate transformation. The finite difference schemes are of second-order accuracy in time and space. The compressible equations are integrated efficiently through the use of a time splitting technique that features a semi-implicit treatment in the vertical for the acoustic modes.

The planetary boundary-layer and free-atmospheric turbulent mixing and diffusion are parameterized using a prognostic equation for the turbulent kinetic energy (TKE), e, budget based on the level 2.5 formulation of Mellor and Yamada (1982) as follows,

$$\frac{\partial e}{\partial t}=-u\frac{\partial e}{\partial x}-v\frac{\partial e}{\partial y}-\dot{\sigma}\frac{\partial e}{\partial \sigma}+BP+SP+D-\varepsilon, \tag{1}$$

where u and v are the horizontal wind velocity components, BP is the buoyancy production, SP is the shear production, D is the subgrid-scale vertical mixing, and ε is the dissipation rate. The buoyancy production is defined as,

$$BP=-\frac{GgK_h}{\theta}\frac{\partial \theta_v}{\partial \sigma}, \tag{2}$$

where G is the coordinate transformation metric defined as $\partial\sigma/\partial z$, g is the acceleration of gravity, K_h is the vertical eddy mixing coefficient for heat, and θ is the potential temperature. The shear production is defined as,

$$SP=K_m\left[\left(G\frac{\partial u}{\partial \sigma}\right)^2+\left(G\frac{\partial v}{\partial \sigma}\right)^2\right], \tag{3}$$

where K_m is the vertical eddy mixing coefficient for momentum. The dissipation rate is parameterized in (1) as,

$$\varepsilon=\frac{\mu}{\ell}e^{3/2}, \tag{4}$$

where μ is a constant of 0.17, and ℓ is a mixing length based on Mellor and Yamada (1982). Accurate representation of the TKE is necessary because the eddy diffusivity coefficients for heat and momentum, K_h and K_m, are directly proportional to $e^{1/2}$. Counter gradient correction terms to the vertical fluxes are included for the potential temperature and water vapor equations. The surface fluxes are computed following the Louis et al. (1982) formulation, which makes use of Monin-Obukhov similarity theory. In the standard application of COAMPS when a predictive ocean-wave model is not used in a tightly coupled manner, z_o is approximated over the open sea by the Charnock relationship (Charnock 1955)

$$z_o=\alpha\frac{\tau}{g\rho}, \tag{5}$$

where τ is the magnitude of the turbulent stress, ρ is the density and α is the Charnock parameter taken to be 0.0185.

A force-restore method is used to parameterize the surface energy budget. Parameterization of short- and long-wave radiation processes, subgrid-scale moist convective processes are included as well. Budget equations for cloud water, cloud ice, raindrops, snow flakes, and water vapor are used to represent the grid-scale evolution of the moist processes. For details of the parameterization methodology, see Hodur (1997) and Hodur and Doyle (1999).

Multivariate optimum interpolation analysis of upper-air sounding, surface, aircraft (ACARS) and satellite data that are quality controlled is the basis for the initial state for the nonhydrostatic model. The Navy Op-

erational Global Analysis and Prediction System (NOGAPS) forecast fields are used for lateral boundary conditions. The application of COAMPS in this type of manner closely emulates a real-time numerical prediction system in spite of the simulations being performed in a hindcast mode. The atmospheric topographic data are based on the U.S. Defense Mapping Agency's 100-m resolution data set.

The atmospheric model is coupled in an interactive mode to the 3rd generation (cycle 4) of the Wave Model (WAM) (WAMDI Group 1988). The quasi-linear theory of wind-wave generation following Janssen et al. (1989) and Janssen (1991) is applied. The transport equation is integrated to solve for the wave variance spectrum for 25 frequencies and 24 directions. The processes represented in WAM include wind-wave interaction, transfer of energy within the wave spectrum, wave propagation and dissipation by whitecapping.

The coupling methodology follows Janssen et al. (1989) and Janssen (1991) and includes the processes represented by mutual interaction of the wind waves and boundary-layer stress. The roughness length used in the coupled simulation is represented by,

$$z_o = \beta \frac{\tau}{g\rho(1-{}^{\tau_w}/_{\tau})^{0.5}}, \tag{6}$$

where τ is the total stress and τ_w is the wave-induced stress. The constant β is chosen as 0.01 implying that (6) reduces to the standard Charnock relationship (5) for a saturated wave state. The wave-induced stress is defined as the integral over all directions and spectral components of the atmospheric momentum flux to the wind-generated wave field (Janssen 1989). It follows that, for a young wind sea, the effective Charnock parameter can be enhanced by an order of magnitude. The simultaneous coupling is physically achieved through communicating the atmospheric stress to the wave model every WAM time step. An iterative technique is then used to calculate τ_w based on the 10-m wind speed, drag coefficient and τ. The new wave-induced Charnock parameter is subsequently used in the Louis et al. (1982) flux calculations in the atmospheric model. This coupling technique using the WAM and an atmospheric model has been applied previously to study air-sea interaction in extratropical cyclones (e.g., Doyle 1995) and tropical cyclones (Bao et al. 2000). The coupling technique is currently being applied operationally at the European Center for Medium Range Forecasts (ECMWF). In this study, the uncoupled simulations are performed with simultaneous integration of the WAM except that the standard Charnock parameter of 0.0185 is used in the atmospheric model flux calculations.

3. Coupled simulations

In this series of simulations, the impact of the wave-induced stress on the evolution of the atmospheric and surface ocean wave fields is investigated. To isolate the importance of the wave coupling, two experiments are performed for each case. The first simulation makes use of the conventional Charnock parameter in the atmosphere and includes a wave simulation based on the atmospheric winds every WAM time step. The second simulation includes the wave-induced stress effects in the modified Charnock formulation following (6) and also includes the feedback of the atmospheric winds, already modified by wave-induced roughness, back to the waves.

Coupled and uncoupled COAMPS/WAM simulations were performed for tropical cyclones Mitch, Bonnie and Bret, and a topographically forced Bora event. A horizontal grid increment of 12 km was used for both COAMPS and the WAM model grids for the Mitch and Bret simulations. Two nested grids were used for the simulations of Bonnie that featured a grid increment of the finest mesh of 6 km and an identical resolu-

tion on the single WAM mesh. The simulation of the Bora event made use of a single mesh with a grid increment of 5 km.

3.1 Tropical Cyclone Mitch Simulations

Tropical cyclone Mitch was responsible for over nine thousand deaths, making it one of the deadliest Atlantic tropical cyclones in history. At the peak intensity, the minimum central pressure was estimated to be 905 hPa with sustained surface wind speed in excess of 80 m s^{-1}, making Mitch the strongest October hurricane in the Atlantic Basin on record.

The simulated central pressure, maximum wind speed at 500 m, maximum significant wave height and maximum Charnock parameter for 0000 UTC 26 October (24-h simulation time) and 0000 27 October (48-h simulation time) 1998 are summarized in Table 1. The central pressure is approximately 8 hPa lower in the coupled simulation than in the uncoupled case. As a result of the enhanced surface stress, the momentum flux increases considerably due to the coupled response. In the parameterization of the surface fluxes, the roughness length for heat is an order of magnitude smaller than that of momentum. Even with this reduction to the roughness length for heat, the wave-induced effects increase the surface heat flux by nearly a factor of 2, from a maximum of 506 W m^{-2} to 946 W m^{-2} at 0000 UTC 27 October. This increase in the heat flux apparently accounts for the 8 hPa reduction in central pressure in the coupled simulation. However, because of the increased drag due to the young ocean waves, the maximum wind speed at 500 m and the surface is less for the coupled simulation. A second coupled simulation was performed with the roughness length for heat and moisture independent of the wave state. The simulated minimum pressure was 941.4 hPa for this coupled simulation, which is 8 hPa higher than the uncoupled simulation and 15 hPa greater than the coupled simulation with the heat and moisture fluxes dependent on the wave state. Clearly, the heat and moisture exchange coefficients appear to have a dominant effect on tropical cyclone intensity relative to momentum flux changes due to wave-induced stress.

As a result of weaker surface winds due to enhanced roughness associated with the young ocean waves, the significant wave height maximum is 2 m less in the coupled simulation, as shown in Table 1 and Fig. 1 for 0000 UTC 27 October. The increased stress associated with the young ocean waves does not appear to have a large impact on the structural character of the ocean wave response. Unfortunately, no observed estimates of the wave fields are available for this time. The Charnock parameter is shown in Fig. 2 for 0000 UTC 26 and 0000 UTC 27 October. The maximum Charnock parameter is 0.32 at 0000 UTC 27 October, which is over an order of magnitude larger than the conventional parameter valid for the open ocean featuring a mature wave state. Also, the Charnock parameter maximum doubles between 0000 UTC 26 and 0000 UTC 27 October coinciding with the time period of rapid intensification of the tropical cyclone (i.e., minimum sea level pressure decreases by 27 hPa in the 33 h period in the coupled simulation). It is noteworthy that the Charnock parameter is a maximum near the eye wall structure coincident with the highest wind speeds and a minimum within the eye. Additionally, the enhanced roughness effects due to the young wave state have a minimal impact on the tropical cyclone track, in spite of the significant changes in the central pressure. For example, at 0000 UTC 27 October (48 h), the position of the tropical cyclone differs by 1 grid point (12 km) in the two simulations.

Variable	Simulation Time	Uncoupled	Coupled	Observed
SLP	24 h	960.1 hPa	958.2 hPa	923 hPa
SLP	48 h	933.6 hPa	925.7 hPa	910 hPa
U_{max}	24 h	62.6 m s^{-1}	59.9 m s^{-1}	67.0 m s^{-1}
U_{max}	48 h	77.0 m s^{-1}	73.8 m s^{-1}	77.0 m s^{-1}
H_s	24 h	14.9 m	13.9 m	
H_s	48 h	17.2 m	15.1 m	
α_{max}	24 h	0.0185	0.18	
α_{max}	48 h	0.0185	0.32	

Table 1. Summary of the simulated central pressure (SLP), 500-m wind speed maximum (U_{max}), significant wave height maximum (H_s) and maximum Charnock parameter value (α_{max}) for tropical cyclone Mitch valid at 0000 UTC 26 October (24 h) and 0000 UTC 27 October 1998 (48 h). Available observed estimates are included.

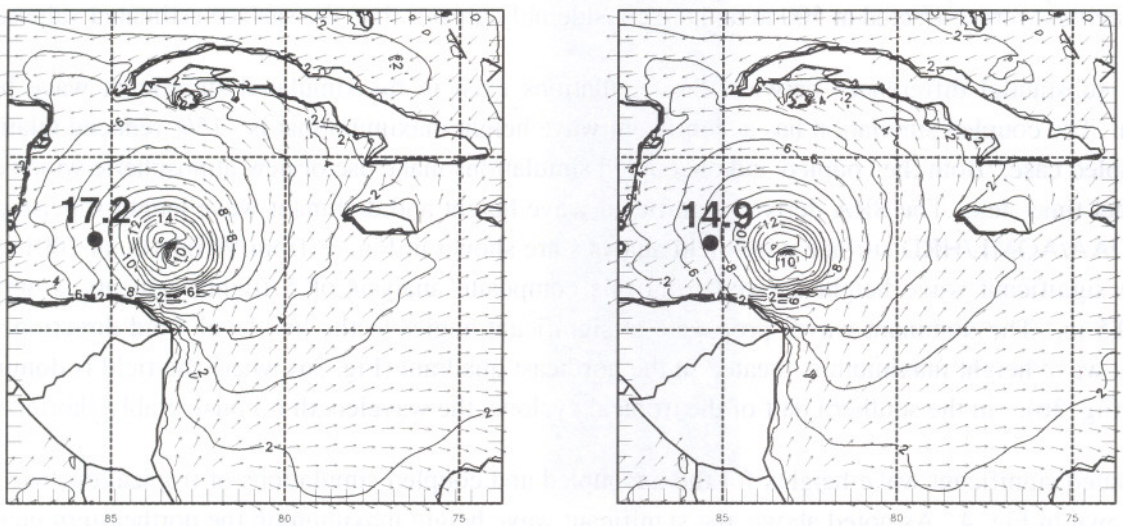

Fig. 1. Significant wave height and direction for a) uncoupled and b) coupled simulations of tropical cyclone Mitch valid at 0000 UTC 27 October 1998 (48-h time).

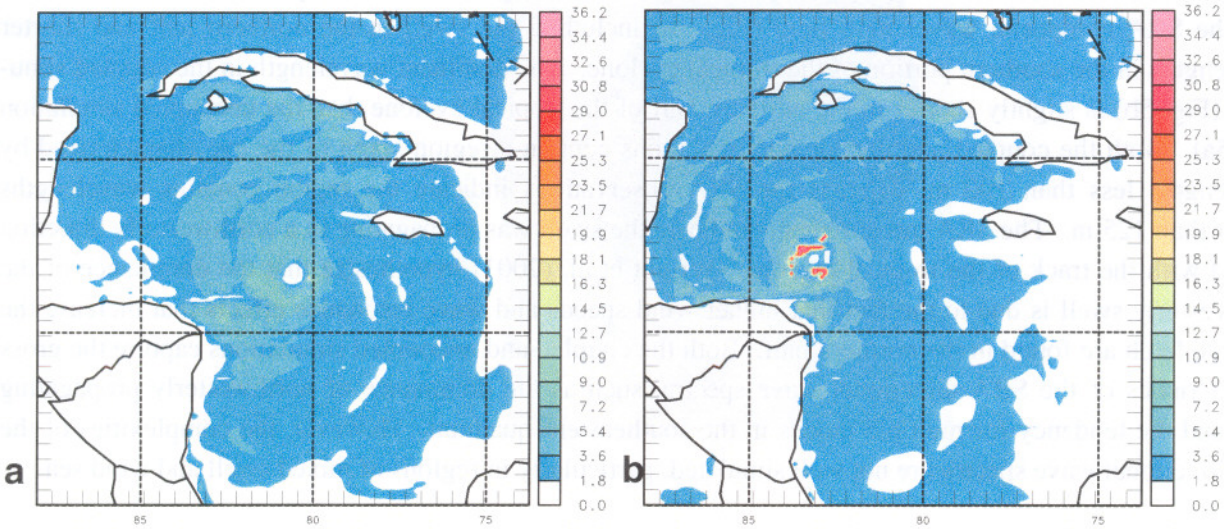

Fig. 2. Charnock parameter ($x10^{-2}$) for tropical cyclone Mitch valid at a) 0000 UTC 26 October 1998 (24-h) and b) a) 0000 UTC 27 October 1998 (48-h).

3.2 Tropical Cyclone Bonnie Simulations

Tropical cyclone Bonnie strengthened to hurricane force at 0600 UTC 22 August 1998 when it was located 400 km north of Hispaniola. Bonnie moved on a general west-northwest heading reaching maximum strength of 51 m s^{-1} and a central pressure of 954 hPa. Eventually, Bonnie made landfall near Wilmington, NC around 0330 UTC 27 August. The focus of this simulation is during an earlier phase of the tropical cyclone on 24 August. On this day, the sea surface directional wave spectrum was measured using the NASA airborne Scanning Radar Altimeter (SRA) carried aboard a NOAA WP-3D hurricane research aircraft at a height of 1.5 km (Wright et. al 2001).

Relevant aspects of the Bonnie simulation for 1200 UTC 24 August (24-h simulation time) and 0000 25 August (36-h simulation time) 1998 are summarized in Table 2. The central pressures for the coupled and uncoupled simulations are quite similar and within 1.5 hPa of each other. However, the observed central pressure is 15-20 hPa deeper than simulated. Once again, the tropical cyclone track is nearly identical between the coupled and uncoupled simulations. Similar maximum velocities are attained in the two simulations. These velocities were extracted at 500 m and are considerably greater than the surface estimated values.

The most substantial differences between the simulations exist in the simulated significant wave height maximum. The coupled simulation has a significant wave height maximum that is ~15% reduced relative to the uncoupled case. Both the coupled and uncoupled simulations make use of new atmospheric winds every wave model time step. The SRA derived significant wave height and dominant wave length superimposed on the NOAA/AOML/HRD surface wind field analysis are shown in Fig. 3 (from Wright et. al 2001). The maximum significant wave height derived from this composite analysis of 5 flight segments is approximately 10.5 m. The dominant waves propagate at significant angles to the low-level wind direction. The significant wave height maximum is located in the northeast quadrant (Fig. 3a) where the field is dominated by swell (Fig. 3b). In the southern half of the tropical cyclone, the wavelength is considerably shorter.

The simulated significant wave heights for the uncoupled and coupled simulations of tropical cyclone Bonnie are shown in Fig. 4. As noted above, the significant wave height maximum in the northeastern quadrant is considerably reduced in the coupled simulation, in spite of the dominance of the swell. The coupled simulation is in overall closer agreement with the SRA derived wave field than the uncoupled case. The dominant wavelength is shown in Fig. 5 for the uncoupled and coupled simulation. Considering the complexity of both the wave and wind fields, the simulated wavelength contains many common characteristics with the SRA composite wavelength field (Fig. 3b) including the swell in the northern half and shorter wavelengths in the southern portion of the tropical cyclone. The dominant wavelength in the coupled simulation (Fig. 5b) is slightly shorter in the northern half of the tropical cyclone than the uncoupled simulation (Fig. 5a). Both the coupled and uncoupled simulations contain a region south of the eye characterized by wavelengths less than 100 m, whereas the SRA observations indicate the region contains wavelengths greater than 125 m. The SRA measurements indicate the swell was propagating in a northwesterly direction aligned with the track of the tropical cyclone. Wright et al. (2001) hypothesize that the dominance of the northwesterly swell is due to the fact that higher wind speeds and wave resonance effects that increase the effective fetch are found in the northern half. Both the coupled and uncoupled simulations capture the gross characteristics of the SRA directional wave spectra, such as the dominance of northwesterly propagating swell and the tendency for multiple modes in the southeastern quadrant. However, the complexities of the SRA directional wave spectra are not well simulated, particularly in regions of mixed swell and wind sea.

Variable	Simulation Time	Uncoupled	Coupled	Observed
SLP	24 h	982.6 hPa	983.2 hPa	962 hPa
SLP	36 h	980.2 hPa	978.7 hPa	964 hPa
U_{max}	24 h	54.1 m s^{-1}	52.2 m s^{-1}	37.0 m s^{-1}
U_{max}	36 h	49.7 m s^{-1}	54.7 m s^{-1}	37.0 m s^{-1}
H_s	24 h	12.8 m	10.9 m	10.5 m
H_s	36 h	12.6 m	11.0 m	
α_{max}	24 h	0.0185	0.15	
α_{max}	36 h	0.0185	0.11	

Table 2. Summary of the simulated central pressure (SLP), 500-m wind speed maximum (U_{max}), significant wave height maximum (H_s) and maximum Charnock parameter value (α_{max}) for tropical cyclone Bonnie valid at 1200 UTC 24 August (24 h) and 0000 UTC 25 August 1998 (36 h). Observed estimates are shown as well.

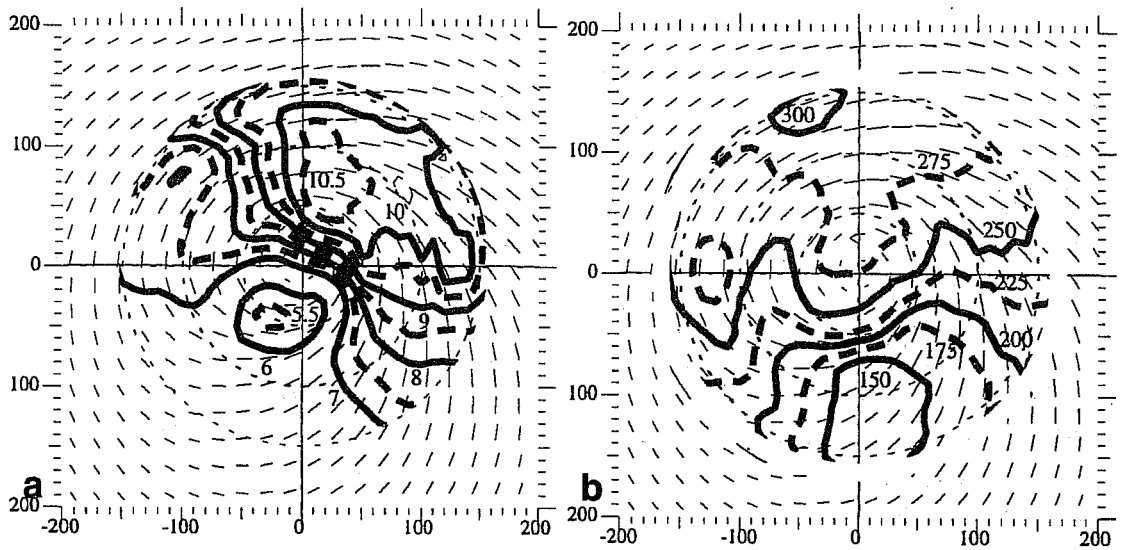

Fig. 3. NASA airborne Scanning Radar Altimeter derived (a) significant wave height (m) and (b) dominant wavelength (m) based on NOAA WP-3D research aircraft data from 24 August 1998 (from Wright et. al 2001).

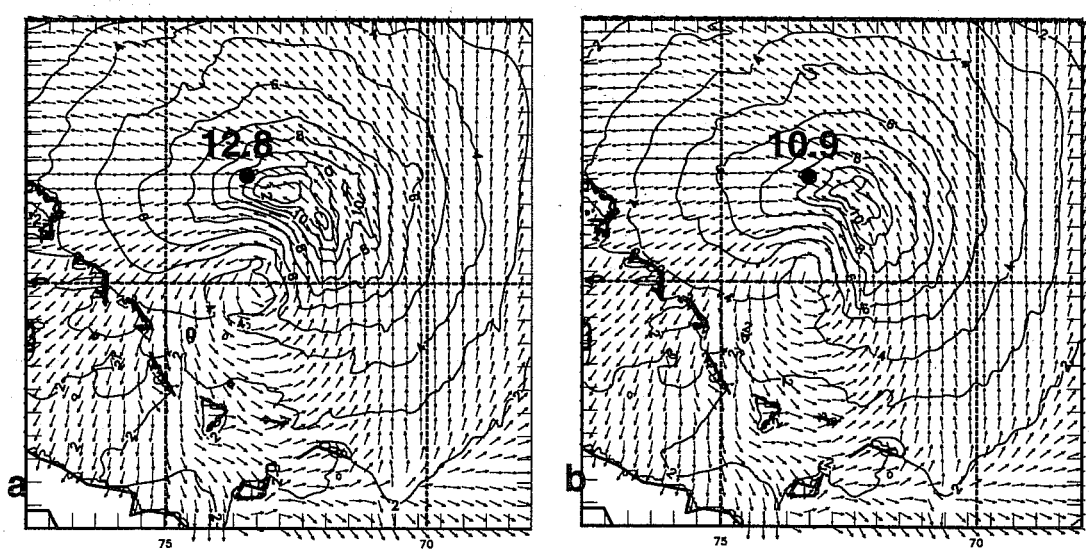

Fig. 4. Simulated significant wave height (m) for the (a) uncoupled and (b) coupled simulations valid at 1200 UTC 24 August 1998 (24 h).

3.3 Tropical Cyclone Bret Simulations

Tropical cyclone Bret was a small hurricane that formed in the Gulf of Mexico and eventually made landfall along the south Texas coast. Near the time of peak intensity, hurricane force winds were confined to a narrow radius of approximately 50 km wide in the northern portion of the cyclone and 25 km to the south.

The simulated characteristics of the atmospheric and wave fields are summarized in Table 3. The central pressure of the tropical cyclone is approximately 3 hPa lower in the coupled simulation than in the uncoupled case, in better agreement with the estimated values based on *in situ* observations. The maximum wind speed at 500 m is similar in both simulations. The significant wave height maximum is ~0.5 m lower in the coupled simulation. The simulated track for Bret is insensitive to any wave coupling issues.

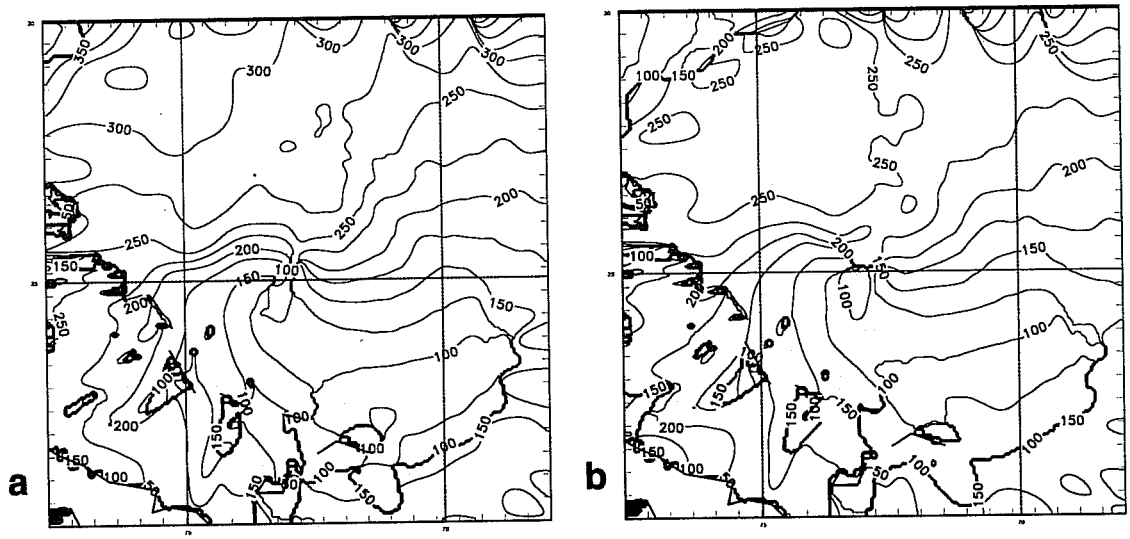

Fig. 5. Wavelength (m) of the wave spectrum peak valid at 1200 UTC 24 August 1998 (24h) for the (a) uncoupled and (b) coupled models.

Variable	Simulation Time	Uncoupled	Coupled	Observed
SLP	24 h	987.2 hPa	983.9 hPa	979 hPa
SLP	48 h	955.2 hPa	952.1 hPa	944 hPa
U_{max}	24 h	45.7 m s^{-1}	47.4 m s^{-1}	41.0 m s^{-1}
U_{max}	48 h	66.9 m s^{-1}	66.2 m s^{-1}	64.0 m s^{-1}
H_s	24 h	8.3 m	7.6 m	
H_s	48 h	12.3 m	11.8 m	
α_{max}	24 h	0.0185	0.10	
α_{max}	48 h	0.0185	0.32	

Table 3. Summary of the simulated central pressure (SLP), 500-m wind speed maximum (U_{max}), significant wave height maximum (H_s) and maximum Charnock parameter value (α_{max}) for tropical cyclone Bret valid at 1200 UTC 21 August (24 h) and 1200 UTC 22 August (48 h) 1999. Available observed estimates are included.

3.4 Bora Event Simulations

The Mesoscale Alpine Programme (MAP) took place during fall 1999 with the objective to measure and understand the meteorology in the vicinity of the Alps. On 7 November 1999, a strong wind event occurred in the lee of the Dnirac Alps of Slovenia and Croatia, often referred to as a Bora. Research aircraft measurements in the low-levels indicate wind speeds were in excess of 30 m s^{-1} along the coast above the Adriatic Sea at 1.5 km.

Coupled and uncoupled simulations of the Bora were performed using COAMPS with a horizontal grid increment of 5 km. The strong downslope winds in the simulation extended westward over the Adriatic and resulted in a significant enhancement to the surface roughness as a result of the growing waves in the fetch-limited conditions, as shown in Fig. 6a. However, in spite of the larger roughness used in the atmospheric model due to the coupled feedback, in general, the simulated atmospheric and wave fields are quite comparable. For example, the wind speed difference at 10 m between the coupled and uncoupled simulations, shown in Fig. 6b, differ by less than 3.0 m s^{-1}, which is comparatively small to the maximum Bora speed of 25 m s^{-1} near the surface. Overall the wave coupling appears to have minimal impact on the atmospheric wind and thermal fields.

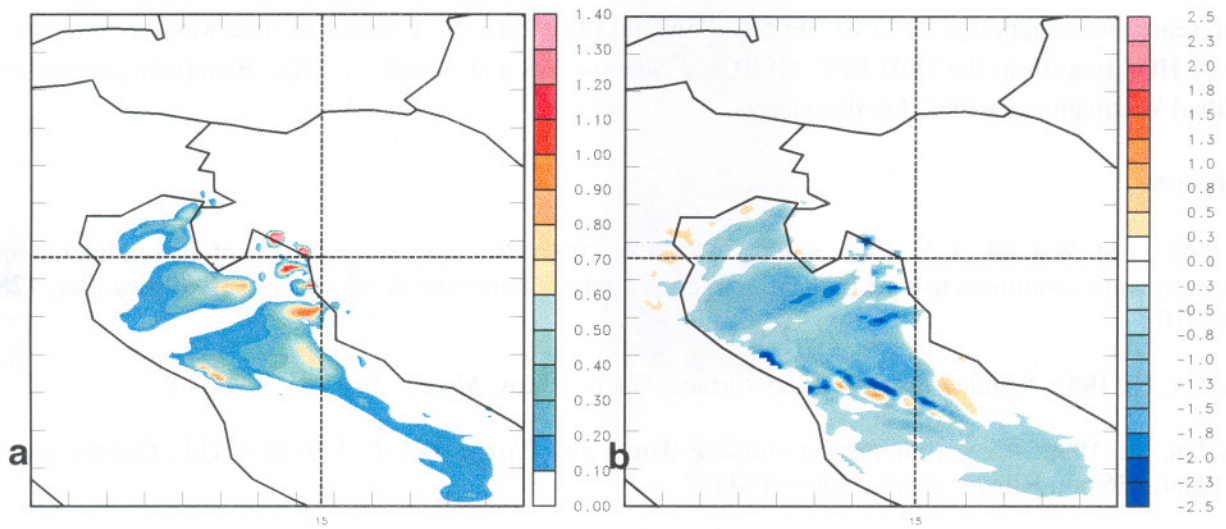

Fig. 6. Simulated (a) roughness length difference (cm) and (b) 10-m wind speed difference (m s^{-1}) between the coupled and uncoupled simulations valid at 1200 UTC 7 November 1999 (12 h).

4. Conclusions

In this study, three major tropical cyclones and a topographically forced Bora event over the Mediterranean Sea were simulated using a coupled atmosphere-ocean surface wave model, COAMPS. The model consists of a nonhydrostatic atmospheric model coupled with the WAM. The models were integrated simultaneously and on identical grids with horizontal grid increments ranging from 12 km to 5 km. The impact of the wave-induced stress was largest for the strongest of the three tropical cyclones, Mitch. The central pressure in the coupled simulation in this particular case was 8 hPa more intense than the uncoupled simulation due to larger surface heat flux effects. This intensification apparently resulted primarily from a weak dependence of the roughness length for heat on the wave state. Other tropical cyclones indicated less sensitivity to wave-induced effects. Significant wave height maxima were typically greater than 10% lower in the coupled simulations. In general, the low-level wind speeds were generally insensitive to the coupling in spite of a Charnock parameter increase by more than a factor of 20. Maximum low-level wind speeds typically were

2-3 m s^{-1} less due to the feedback of ocean wave-induced stress. However, local differences in excess of 10 m s^{-1} were found. The tracks of the tropical cyclones were especially insensitive to wave coupling effects. Topographically forced flows in the coastal zone, such as the Bora, are characterized by occasionally high near-surface wind speeds and fetch-limited conditions. However, in this study, the Bora event was least sensitive to the ocean wave enhanced roughness of all the cases considered. For example, in spite of a substantial increase in the surface roughness associated with the young ocean waves, the near-surface wind speeds differ by less than 3 m s^{-1} between the uncoupled and coupled simulations.

Several issues remain unresolved with respect to air-sea interaction in high wind conditions. The accuracy of wind energy transfer, dissipation and nonlinearity representations in wave models, surface flux exchange at the air-sea interface in atmospheric models, and air-ocean coupling methodologies need to be assessed. In the high wind regime in particular, gustiness effects and mesoscale transients need to be considered in order to improve surface wind stress forcing. An improved representation of the bulk effect of sea spray on the fluxes of heat and moisture may be required before realistic simulations of air-sea interaction at high wind speeds can be achieved.

Acknowledgements

This research was supported by ONR PE0602435N and PE0601153N. Computing time was supported by a grant of HPC time from the DoD HPC MSRCs at Stennis, MS and Aberdeen, MD. Beneficial discussions with Paul Wittmann contributed to this study.

References

Bao, J.-W., J.M. Wilczak, J.-K. Choi, and L.H. Kantha, 2000: Numerical simulations of air-sea interaction under high wind conditions using a coupled model: A study of hurricane development. *Mon. Wea. Rev*, **128**, 2190-2210.

Charnock, H., 1955: Wind stress on a water surface. Quart. J. Roy. Meteor. Soc., 81, 639-640.

Donnelan, M., 1990: Air sea interaction. *Surface Waves and Fluxes, Vol. 1.* Edited by G.L. Geernaert and W.J. Plant, 336 pp., Kluwer Acad., Norwell Mass.

Doyle, J. D., 1995: Coupled ocean wave/atmosphere mesoscale model simulations of cyclogenesis. *Tellus*, **47A**, 766-788.

Hodur, R.M., 1997: The Naval Research Laboratory's Coupled Ocean/Atmosphere Mesoscale Prediction System (COAMPS). *Mon. Wea. Rev.*, **125**, 1414-1430.

Hodur, R. M., and J. D. Doyle, 1999: The coupled ocean/atmosphere mesoscale model prediction system (COAMPS). *Coastal Ocean Prediction*, Coastal and Estuarine Studies 56, 125-155.

Janssen, P.A.E.M., 1989: Wave-induced stress and the drag of air flow over sea waves. *J. Phys. Oceanogr.*, **19**, 745-754.

Janssen, P.A.E.M., 1991: Quasi-linear theory of wind-wave generation applied to wave forecasting. *J. Phys. Oceanogr.*, **21**, 1631-1642.

Kepert, J.D, C.W. Fairall and J.W. Bao, 1999: Modelling the interaction between the atmospheric boundary layer and evaporating sea spray droplets. *Air-Sea Fluxes of Momentum, Heat and Chemicals.* editor G.L Geeraert. Kluwer.

Louis, J.F., M. Tiedtke, and J.F. Geleyn, 1982: A short history of the operational PBL-parameterization at ECMWF. *Workshop on Planetary Boundary Layer Parameterization.* ECMWF, Reading, 59-79.

Mellor, G.L. and T. Yamada, 1982: Development of a turbulence closure for geophysical fluid problems. *Rev. Geophys. and Space Phys.*, **20**, 851-875,

Smith, S.D., R.J. Anderson, W.A. Oost, C. Kraan, N. Maat, J. De Cosmo, K.B. Katsaros, K. Davidson, K. Bumke, L. Hasse, and H.M. Chadwick, 1992: Sea surface wind stress and drag coefficients. The HEXOS results. *Bound-layer Meteor.*, **60**, 109-142.

The WAMDI Group (S. Hasselmann et al.), 1988: The WAM model - a third generation ocean wave prediction model. *J. Phys. Oceanogr.*, **18**, 1775-1810.

Wright, W., E.J. Walsh, D. Vandemark, W.B. Krabill, A.W. Garcia, S.H. Houston, M.D. Powell, P.G. Black, and F.D. Marks, 2001: Hurricane direction wave spectrum variation in the open ocean. Submitted to *J. Phys. Oceanogr.*